LA-7562

Low-Noise Audio Amplifiers and Preamplifier for Use with Intrinsic Thermocouples

LOS ALAMOS SCIENTIFIC LABORATORY
Post Office Box 1663 Los Alamos, New Mexico 87545

LA-7562
UC-37
Issued: March 1979

Low-Noise Audio Amplifiers and Preamplifier for Use with Intrinsic Thermocouples

Gerald C. Langner
Robert D. Sachs
Fred L. Stewart

LOW-NOISE AUDIO AMPLIFIERS AND PREAMPLIFIER FOR USE WITH INTRINSIC THERMOCOUPLES

by

Gerald C. Langner, Robert D. Sachs, and Fred L. Stewart

ABSTRACT

Two simple, low-noise audio amplifiers and one low-noise preamplifier for use with intrinsic thermocouples were designed, built, and tested. The amplifiers and the preamplifier have different front end designs. One amplifier uses ultralow-noise operational amplifiers; the other amplifier uses a hybrid component. The preamplifier uses ultralow-noise discrete components. The amplifiers' equivalent noise inputs, at maximum gain, are 4.09 nV and 50 nV; the preamplifier's input is 4.05 μV. Their bandwidths are 15 600 Hz, 550 Hz, and 174 kHz, respectively. The amplifiers' equivalent noise inputs were measured from ~0 to 100 Hz, whereas the preamplifier's equivalent noise input was measured from ~0 to 174 kHz.

I. INTRODUCTION

We designed, built, and tested two low-noise audio-frequency voltage amplifiers and one low-noise preamplifier (preamp) for use with intrinsic thermocouples. An intrinsic thermocouple does not use electronic "ice points" or an ice bath reference junction potential, but instead develops a *floating* junction potential between its two ends (typically 10^{-6} V/°C at room temperature) while being heated. Group M-1 at the Los Alamos Scientific Laboratory (LASL) uses intrinsic thermocouples (Fig. 1) to measure the thermal transient responses of SERAPH (formerly TREAT) nuclear reactor fuel pins.

Thermocouple response times, which depend upon the sample and thermocouple materials being used, can be calculated to the 95% level of maximum temperature rise.[1] Response times for a 10-mil-diam chromel-alumel thermocouple wire range from ~2 to 10 ms, as compared with ~500 μs to ~1 ms for a 5-mil-diam wire.

Figure 2 shows the cross section of an intrinsic thermocouple used at LASL for determining thermal properties of fuel elements that have a central bore. The thermocouple consists of two small-diameter stainless steel tubes, one inserted into the other. The Teflon-coated chromel and alumel wires that run through the inner tube are epoxyed to the inside of the tube ends. On the sensing end of the tube, the wires are fed into holes bored through a Lucite head that is epoxyed to the outer tube. The Lucite head is the same diameter as the outer tube. A sliding motion of the steel tubing extends or retracts the thermocouple wires through the Lucite head. Beads of solder prevent dislodging of the inner tube from the Lucite head. The two surface wires are shielded from heat and other sources of radiation

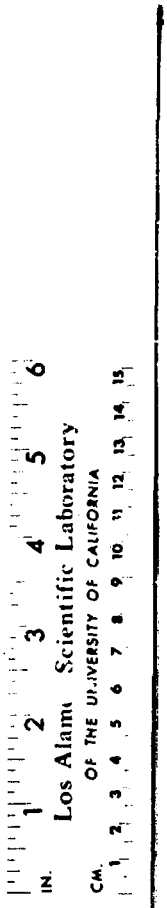

Fig. 1.
Intrinsic thermocouple used by LASL Group M-1.

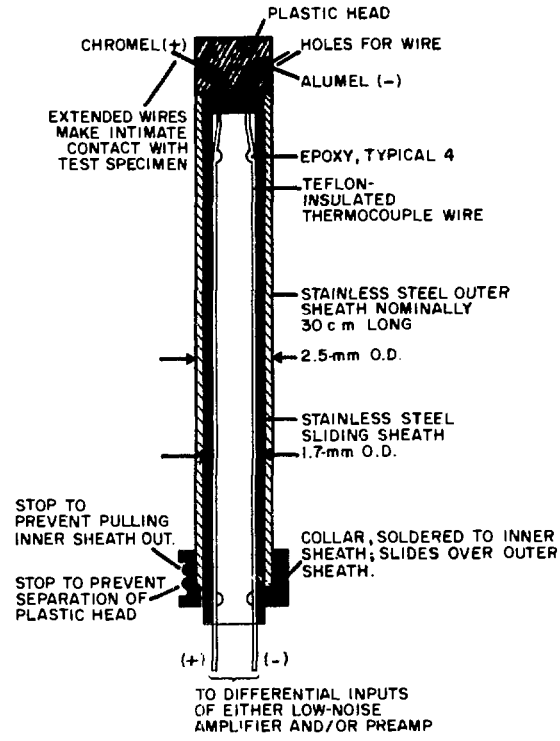

Fig. 2.
Cross section of an intrinsic thermocouple. Note: Sheaths are made from hypodermic tubing.

by a long stainless steel tube. The two thermocouple lead wires are attached to the instrumentation amplifier's input stage, which is a direct-coupled, differential input amplifier with internal feedback for voltage gain.

II. DESCRIPTION OF LOW-NOISE AMPLIFIERS AND PREAMPLIFIER

A. Low-Noise Amplifier No. 1 (LNA 1)

The LNA 1 design schematic is shown in Fig. 3. The 10 K-ohm resistors across the Burr-Brown (BB) 3620 K inputs (see instrumentation amplifier—yellow area in Fig. 3) are connected to the lead wires of an intrinsic thermocouple. The resistors allow

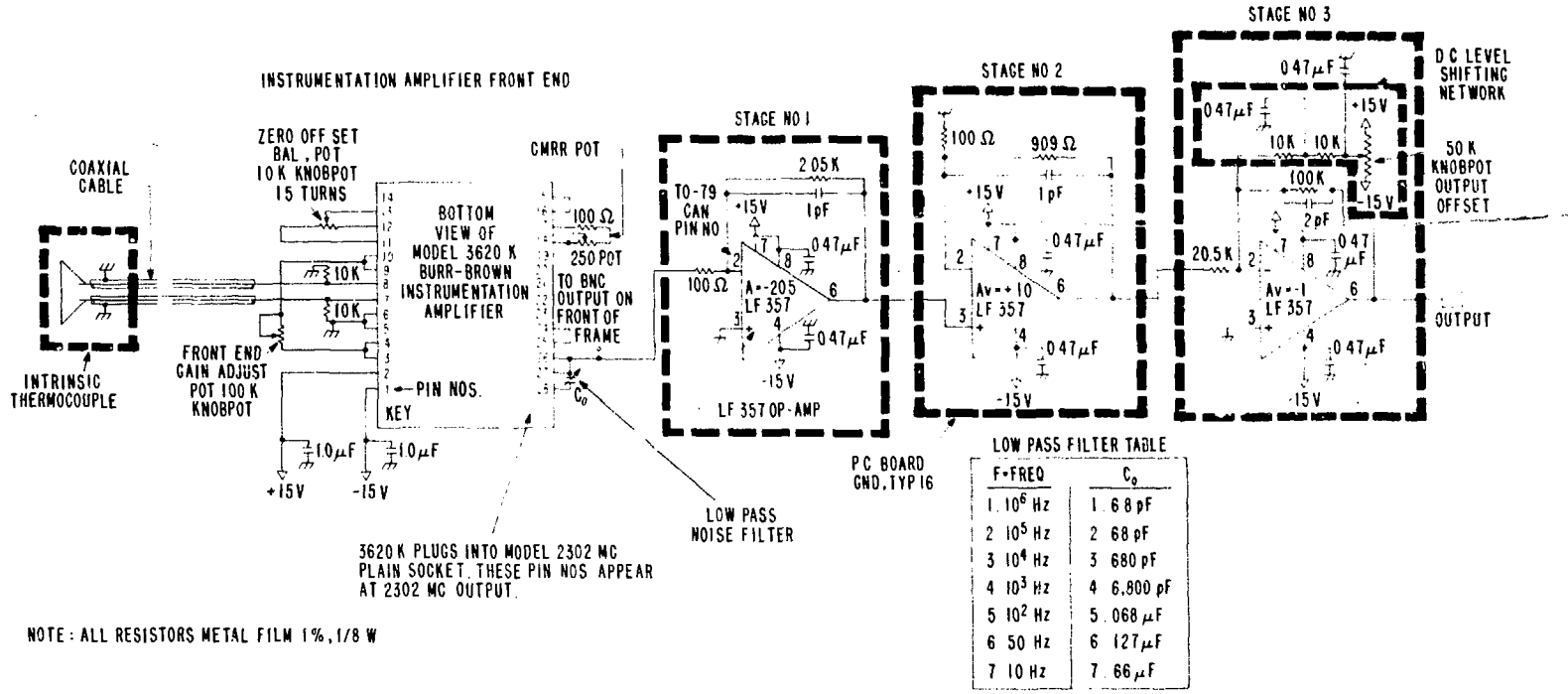

Fig. 3.
LNA 1 design schematic.

bias currents to flow through the BB 3620 K inputs.[2] The BB 3620 K voltage gain is adjustable from 0.0 to 725 V/V. The low pass filter (LPF) capacitor groups allow the upper −3-dB break frequency to range from 10 Hz to the BB 3620 K's upper break frequency.

The BB 3620 K output is connected to a transresistive amplifier (Stage 1—black area in Fig. 3) that has a closed-loop voltage gain of −20.5 and uses a National Semiconductor LF 357 Bifet operational amplifier* that has high input impedance, junction field effect transistors (JFETs), low (bipolar) transistor output impedance, and an excellent overall low-noise capability.[3] The LF 357 noninverting input can be connected directly to ground because of its JFET input. A 1-pF capacitor, in parallel with a 2050-ohm resistor, prevents high-frequency parasitic oscillations from appearing at the LF 357 output (pin 6). Parasitic oscillations are undesirable middle- and high-frequency oscillations that usually appear (sometimes with no input signal applied) at high open-loop gain amplifiers, voltage comparators, and other devices.

The Stage 2 input (blue area in Fig. 3) is connected directly to the Stage 1 (pin 6) output. Stage 2 uses a voltage amplifier configuration with a closed-loop voltage gain of approximately +10. It uses an LF 157 and a 1-pF capacitor, in parallel with a 909-ohm resistor, to prevent high-frequency parasitic oscillations. Its output is connected to a large coupling capacitor to suppress direct current (dc) voltage drifts and dc flow (around the feedback resistors) from Stage 2 to Stage 3.

Stage 3 (red area in Fig. 3) uses a transresistive configuration** with a closed-loop voltage gain of approximately −1. A dc bias, or level-shifting, circuitry (note green area in Fig. 3) makes the final dc output adjustable to be compatible with an analog-to-digital converter.

We designed the two amplifiers and the preamp such that their voltage gains decrease from the first to the final stage. This is common in low-noise designs.[5]

*Bifet operational amplifers (op-amps) are so-named because of their *bi*polar transistor output and their *f*ield effect *t*ransistor (FET) inputs.

**The four basic feedback configurations commonly used around amplifier stage(s) or operational amplifier(s) are voltage, current, transresistive, and transconductance.[4]

The 350-μF capacitors on the BB 3620 K inputs reduce the input low-frequency noise components, and a metal shield around the BB 3620 K suppresses other noise. Low-frequency noise is common to transistors, diodes, thermisters, thermocouples, etc., and is produced (in transistors) by the trapping and detrapping of carriers in surface energy states.

Figure 4 shows the LNA 1 with its outer shield cover removed. Also shown is the shielded BB 3620 K, as well as the other stages. The dc power supply for both amplifier designs is located in another shielded enclosure.

B. Low-Noise Amplifier No. 2 (LNA 2)

The LNA 2 (Fig. 5) has 100-μF capacitors connected to both front end inputs for low-frequency noise suppression and uses an instrumentation amplifier (Stage 1) configuration (yellow area in Fig. 5) with LM381AN and LF 357A active devices. We chose the LM381AN because it can be biased in an

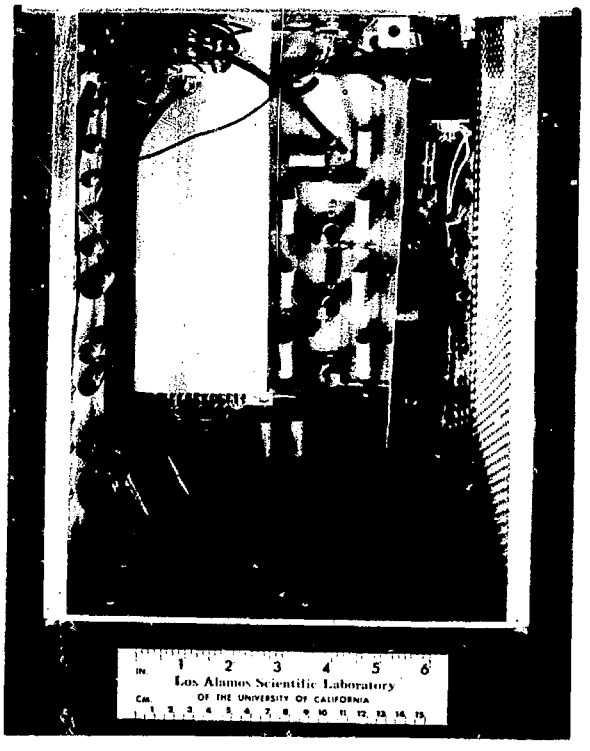

Fig. 4.
LNA 1 with its outer shield cover removed.

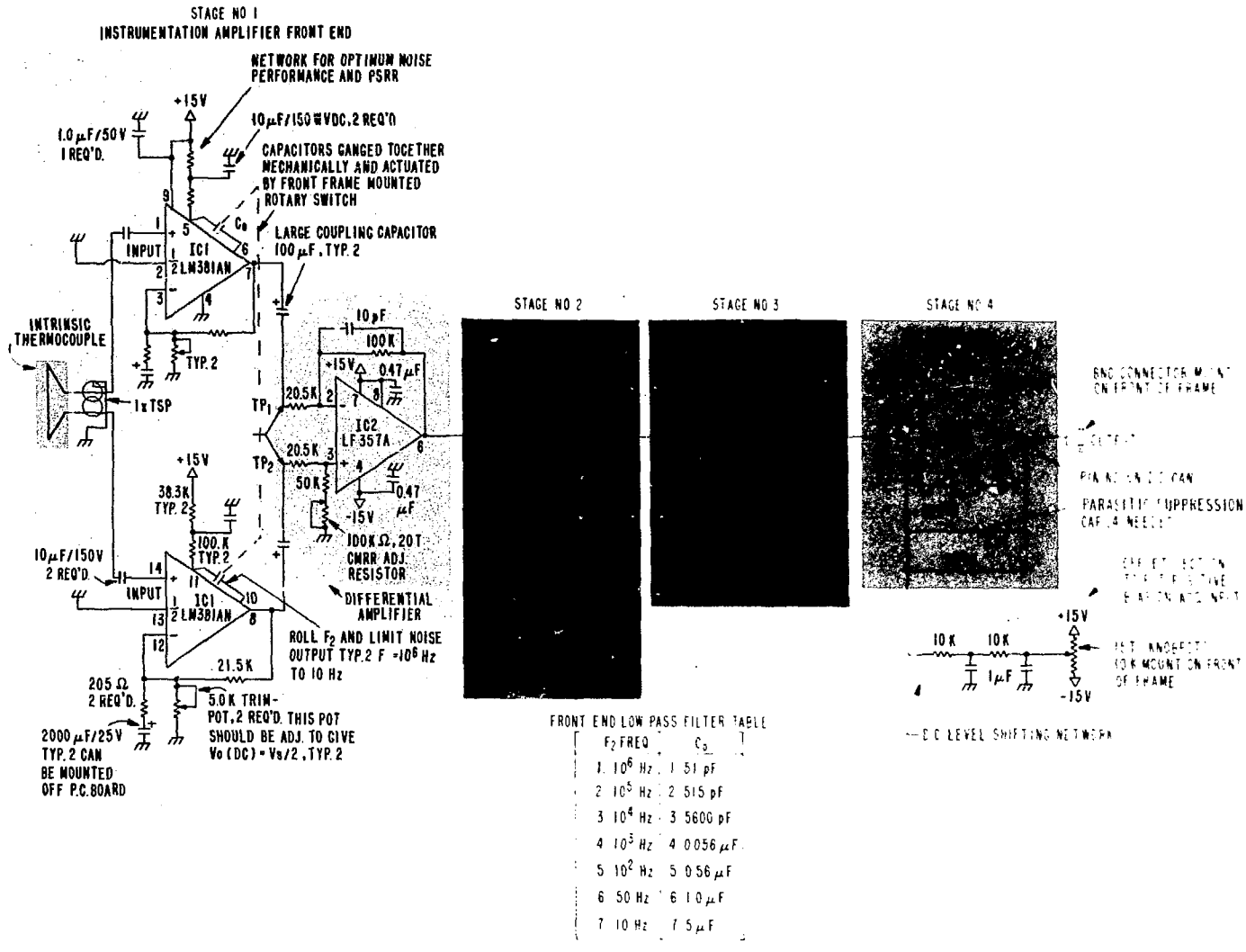

FRONT END LOW PASS FILTER TABLE

	F_2 FREQ	C_2
1	10^6 Hz	1 51 pF
2	10^5 Hz	2 515 pF
3	10^4 Hz	3 5600 pF
4	10^3 Hz	4 0056 μF
5	10^2 Hz	5 0.56 μF
6	50 Hz	6 1.0 μF
7	10 Hz	7 5 μF

Fig. 5.
LNA 2 design schematic.

ultralow-noise state while simultaneously obtaining a large power supply rejection ratio (PSRR).[6] A PSRR, which is similar to a CMRR,* can be defined as PSRR = ΔV supply/ΔV output.

The National Semiconductor LM381AN contains two independent ultralow-noise preamps with connections to couple the LPFs that control the upper −3-dB break frequency for both channels, thus limiting the LM381AN output noise bandwidth.

Each LM381AN channel is configured as a voltage amplifier with a closed-loop voltage gain of approximately +100 and uses multiturn potentiometers (pots) in the feedback loops to set the dc levels, and slightly affect alternating current (ac) gain, out of each channel. The low-noise biasing network (shown above each channel amplifier in Fig. 5) optimizes the currents in the LM381AN front end internal transistors, thus producing very low noise outputs and maximizing the PSRR.

The 2000-μF capacitor in series with a 205-ohm resistor (note feedback loop) primarily determines the lower −3-dB break frequency of the two identical front end amplifiers. The front end amplifiers' outputs (pins 7 and 8) go to the inputs of a differential amplifier (pink area in Fig. 5) through 100-μF coupling capacitors to suppress unequal dc levels from the input amplifier's outputs.

The differential amplifier, configured around an LF 357A op-amp with a 10 K-ohm pot in the resistor string connected to the noninverting input (of the LF 357A), adjusts the common mode rejection ratio (CMRR). The differential amplifier has a closed-loop differential voltage gain of +10, whose output (pin 6) is connected to a variable gain transresistive amplifier (Stage 2) with a closed-loop voltage gain spread from −1 to −11 V/V.

Stage 2 (blue area in Fig. 5) uses an LF 357A or LF 157 op-amp active device, whose ac output (pin 6) goes to Stage 3 (red area in Fig. 5). Stage 3 is another transresistive amplifier with a closed-loop voltage gain of −20.5. The 100-μF coupling capacitor is used to isolate dc levels.

The Stage 3 output (pin 6) goes to the final Stage 4 (green area in Fig. 5), which is configured as a transresistive amplifier with a closed-loop voltage gain of −1.0. The Stage 4 bias network (orange area below Stage 4 in Fig. 5) has the same function as in LNA 1.

All stage amplifiers, front ends, etc., on all low-noise designs use many decoupling and by-pass capacitors to prevent "motor boating" and/or parasitic oscillations. (Motor boating is an electronic jargon term that refers to low-frequency oscillations that can result from inadequate filtering in the dc circuits.[4])

In our amplifier and preamp designs, we used metal film resistors and polystyrene capacitors, such as front end LPF capacitors, in critical locations to reduce the noise output.[5,7]

We did not use high-frequency techniques such as ground plane(s) or short lead lengths in the LNA 1, but we used a double-sided ground plane to suppress parasitic oscillations and distorted signals from the LNA 2 front end (yellow area in Fig. 5). A double-sided ground plane is produced by filling in all unused printed circuit (pc) board areas with copper on both sides of the board and grounding all the copper. Both designs required large pc boards because of the large-coupling and by-pass capacitors that were used.

Because we found the hybrid and monolithic front ends easy to design with, we did not consider a modified rush preamp-differential amplifier combination, parallel stage amplifiers, cascode inputs, etc.[8]

Figure 6 shows the LNA 2 with its outer shield cover removed.

C. Low-Noise Instrumentation Preamplifier

The low-noise instrumentation preamp (Fig. 7) uses two closely matched 2N6550 N-Channel ultralow-noise JFETs and an LF 157.[9] The two 2N6550 JFETs were chosen because of their extremely low-noise characteristics and their high transconductance (for example, g_m = 20 000 μmho) near their zero temperature coefficients (ZTCs).

We used a Tektronix 577 transistor curve tracer to pick the two closest matching 2N6550 JFETs (out of seven available) and to determine the ZTC drain currents, I_{DZ}.[10] (I_{DZ} is the dc drain current that biases a JFET so that its drain current and other parameters are temperature independent.[11])

*CMRR (ΔV inputs/ΔV output) is a measure of a differential amplifier's capability to subtract out common mode (or identical signals) applied to its inputs. With an infinite CMRR, *no* output signal would be observed for identical signals at the amplifier's inputs.[4]

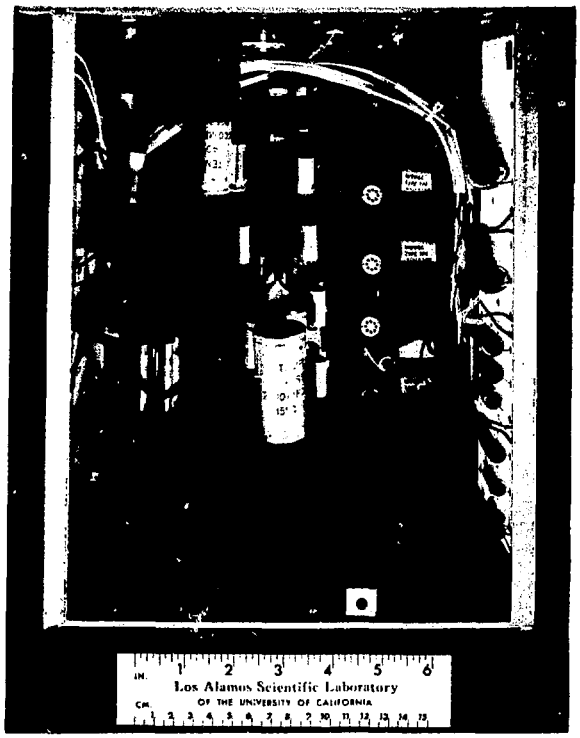

Fig. 6.
LNA 2 with its outer shield cover removed. Note: All active devices have been removed.

The 2N6550 JFETs used an unbypassed common source configuration (red and blue areas in Fig. 7) and self-biasing networks to negate the use of large by-pass capacitors. Each JFET produced an incremental small signal voltage gain of $A_v \cong -40$. The pots in the drain strings were used to equalize the voltage gain. The 100-μF capacitors coupled the amplified signals from the two JFETs to the input of the differential amplifier, which used an LF 157. Large coupling capacitors were needed to attain a low −3-dB break frequency.

To obtain a higher transconductance, g_m, the JFETs were dc biased slightly above their ZTCs, with their respective ac coupled outputs going to the input resistors of the differential amplifier (black area in Fig. 7). The differential amplifier has a CMRR network connected to its positive input.

To reduce the system output noise and equivalent noise input (ENI), the preamp's differential voltage gain was approximately A_v = 1680 V/V. Outside noise was reduced by placing the preamp inside an aluminum/mu metal box, which was built for easy assembly and disassembly. Figure 8 shows the low-noise instrumentation preamp with its outer shield cover removed.

III. PERFORMANCE OF THE TWO LOW-NOISE AMPLIFIERS AND PREAMPLIFIER

In Appendix A we describe the sine-wave method that we used to determine the noise characteristics of the amplifiers and the preamp. We used this method because a commercial noise analyzer was not available.[5] Noise measurements for both amplifiers and the preamp were made with *both* their inputs shorted to ground.

We used the sine-wave method and pulse tilt method, respectively, (see Appendix A) to measure the upper (f_2) and lower (f_1) −3-dB break frequencies (with one input to both amplifiers and preamp shorted to ground). The lower −3-dB break frequency, f_1, was calculated from the equation $f \cong pf/\pi \times 100\%$, where p is the percentage tilt of the test square wave and f is the frequency of the test square wave.[12]

The upper break frequencies for LNA 1, LNA 2, and the preamp were 15 600 Hz, 550 Hz, and 174 kHz, respectively; their respective low break frequencies were 0.995 Hz, 1.59 Hz, and 0.959 Hz.

The experimental voltage ENIs, with *both* inputs grounded and at maximum gain, for LNA 1, LNA 2, and the preamp were 4.09 nV, 50 nV, and 4.05 μV, respectively. The amplifiers' ENIs were measured from ~0 to 100 Hz, whereas the preamp's ENI was measured from ~0 Hz to 174 kHz. (Industry has not established standards for comparing the noise characteristics of amplifiers with differential or instrumentation amplifier front ends, but typically output noise is measured with *both* inputs shorted to ground.) The measured output noise, with both inputs shorted to ground, for LNA 1, LNA 2, and the preamp was 0.0012 V, 0.001 V, and 0.0034 V, respectively, and the maximum transfer voltage gains were 2.9×10^6 V/V, 2.0×10^4 V/V, and 1.68×10^3 V/V, respectively.

Table I shows the experimental performance characteristics (including noise) for the LNA 1, LNA 2, and preamp. The measured front end

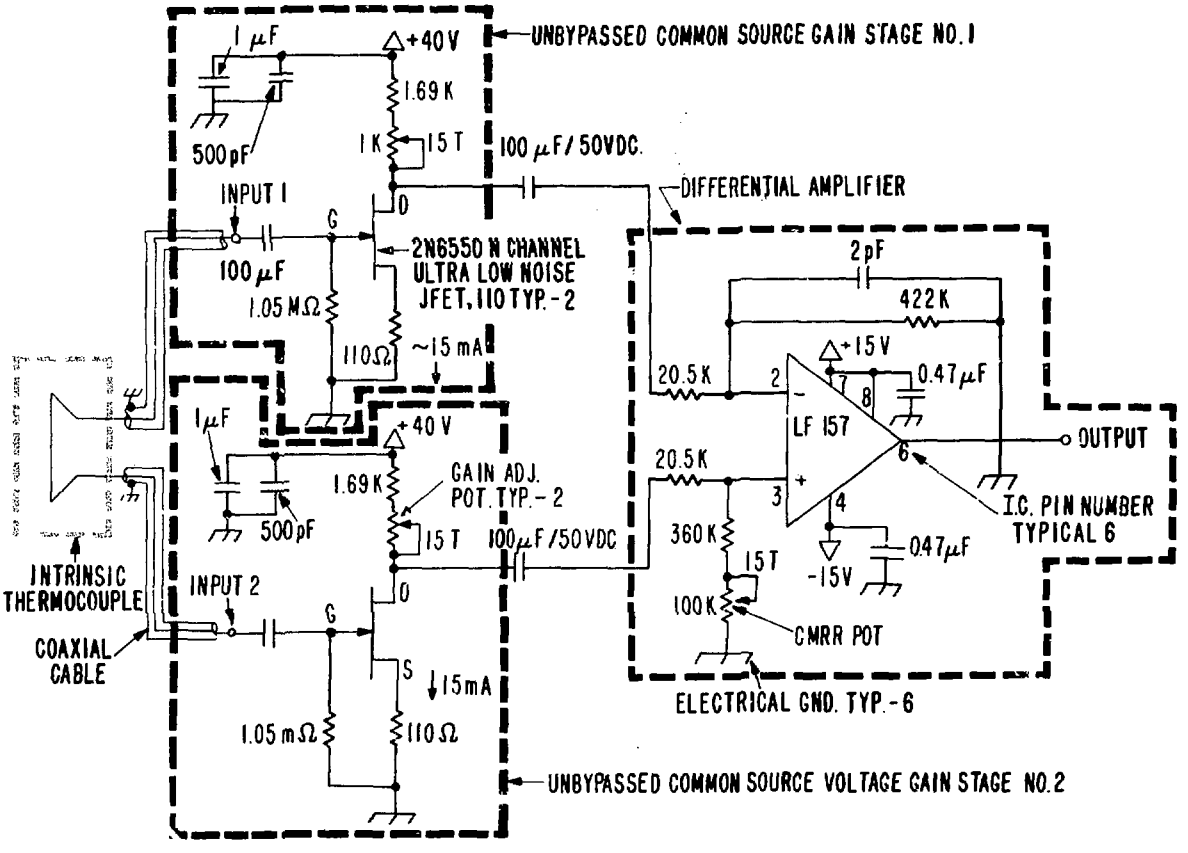

Fig. 7.

Low-noise instrumentation preamp schematic. Note: All resistors are metal film.

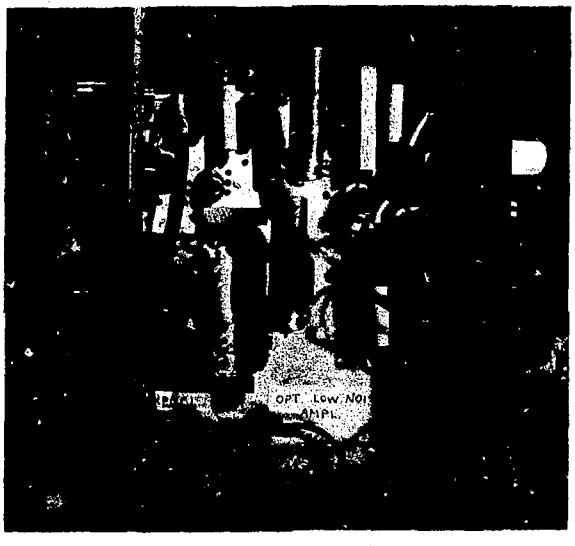

Fig. 8.

Low-noise instrumentation preamp with its outer shield cover removed.

TABLE I

EXPERIMENTAL PERFORMANCE CHARACTERISTICS

	LNA 1	LNA 2	Preamp
Maximum transfer voltage gain	290 290 V/V	20 000 V/V	1680 V/V
Front end CMRR	100 dB	70 dB	68 dB
Total output noise[a]	0.0012 V rms	0.001 V rms	0.0034 V rms
ENI from sine-wave method[a,b]	4.09 nV	50 nV	4.05 μV
Upper −3-dB break frequency[c]	15 600 Hz	550 Hz	174 kHz
Lower −3-dB break frequency[d]	0.995 Hz	1.59 Hz	0.959 Hz

[a]Total output noise and ENI were measured with *both* inputs shorted to ground and calculated using the *maximum* transfer voltage gain, K_t.

[b]The ENIs for LNA 1 and LNA 2 were measured from ~0 to 100 Hz, whereas the preamp's ENI was measured from ~0 Hz to 174 kHz.

[c]One input to amplifier and/or preamp grounded. Also, the LPFs are set at the *highest frequency* for LNA 1 and LNA 2 when measuring the upper break frequency.

[d]One input to amplifier and/or preamp grounded.

CMRR for LNA 1 (100 dB), compared with 70 dB for LNA 2 and 68 dB for the preamp, indicates that the LNA 1 would perform better at rejecting external noise.

Some amplifier theoretical noise calculations are presented in Appendix B.

IV. CONCLUSIONS AND RECOMMENDATIONS

The LNA 1 has a better front end CMRR than either the LNA 2 or the preamp. The low −3-dB break frequency of the LNA 1 is slightly less than that of the LNA 2, and its upper −3-dB break frequency is larger than that of the LNA 2. Because of the precision-trimmed resistors inside the BB 3620 K, the LNA 1's CMRR (100 dB) is far greater than the CMRR of the LNA 2 or the preamp. Also, it is rarely possible to have *exactly* the same signals occurring simultaneously at the differential inputs of the LNA 2 and the preamp, even when using front end gain pots.

The low-noise characteristics of the LNA 1 (Table I) are superior to those of the LNA 2, but its total component cost is more than that of the LNA 2.

The maximum transfer voltage gains obtainable from the LNA 1, LNA 2, and preamp were 2.9×10^5 V/V, 2.0×10^4 V/V, and 1.68×10^5 V/V, respectively.

Noise (and amplifier) bandwidth limiting, using the LPF capacitors, was necessary, as is evident from Fig. 9(a), which shows an output dc signal from the LNA 1 with a 10-Hz noise bandwidth. Figure 9(b) shows that the same dc signal with a 10-kHz noise bandwidth is almost obscured in the noise.

The LNA 1, LNA 2, and preamp all perform excellently with intrinsic thermocouples connected to their inputs. The output bias circuitry in the LNA 1 and LNA 2 allows direct connection to analog-to-digital converters.

Measurements of the instrumentation preamp's (Fig. 7) noise and other characteristics show that because of the extremely low 2N6550 noise properties, the preamp's circuit has a low ENI over its 174-kHz bandwidth.

We recommend the use of LNA 1 over LNA 2 because of its better performance characteristics (see Table I), shorter debugging time, and simple design. In addition to its short construction time, very short debugging time, and simple design, the preamp also shows some superior performance

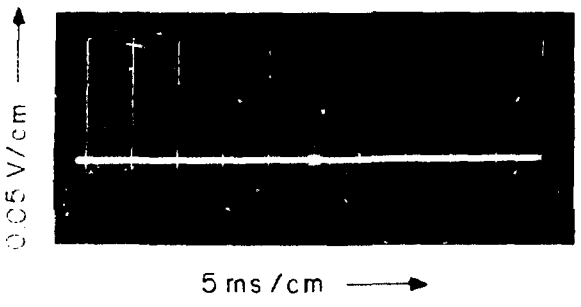

(a) 10-Hz noise bandwidth.

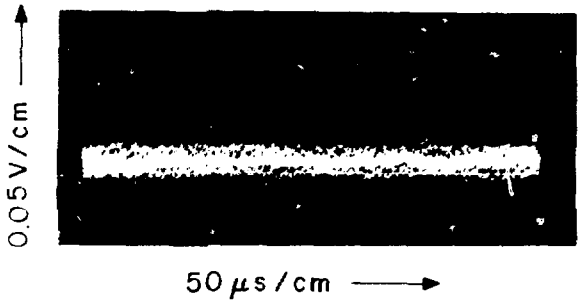

(b) 10-kHz noise bandwidth.

Fig. 9.
Oscilloscope photographs of the output from the LNA 1 showing noise on the dc signal.

characteristics (see Table I) when compared with those of the amplifiers.

Some explanations of the differences in the experimental results are as follows.

- External noise was picked up during the experimental measurements.
- Cross-talk occurred between the LM381AN channels.
- There were sine-wave test generator amplitude variations.
- There were dc drifts in the HP3400A true rms voltmeter.
- The preamp and amplifiers are inherently different.
- There was microphonic noise generated in the various coaxial cables connecting the sine-wave test system.

APPENDIX A

NOISE MEASUREMENT TECHNIQUES

I. NOISE GENERATOR METHOD

Figure A-1(a) shows the block diagram of the noise generator method experiment, where

R_s = voltage source resistance,
E_{ni} = amplifier equivalent input noise or equivalent noise input (ENI),
E_{no} = amplifier output noise, and
E_{ns} = calibrated noise source.

With E_{ns} connected, $E_{no} = E_{no_1}$.

$E_{no_1}^2 = K_t^2 (E_{ni}^2 + E_{ns}^2)$.*

where K_t is transfer voltage gain.

With E_{ns} disconnected, $E_{no} = E_{no_2}$.

$E_{no_2}^2 = K_t^2 E_{ni}^2$.

*Noise quantities usually are shown squared because the power from uncorrelated noise sources is additive.

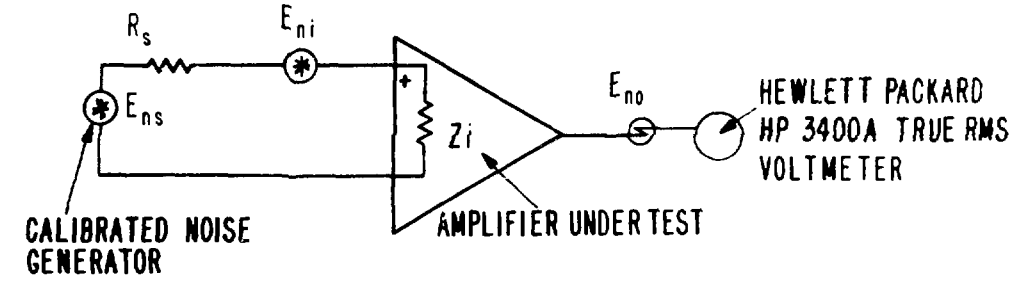

(a) NOISE GENERATOR METHOD

Fig. A-1.
Noise measuring techniques. Note: Either input could be grounded on the above amplifiers.

Thus,

$$E_{ni}^2 = \frac{E_{no_2}^2}{K_t^2} = \frac{E_{no_2}^2 E_{ng}^2}{E_{no_1}^2 - E_{no_2}^2} \quad \text{, and if } E_{no_1}^2 = 2E_{no_2}^2 \text{ ,}$$

$$E_{ni}^2 = \frac{E_{no_2}^2 E_{ng}^2}{E_{no_1}^2 - E_{no_2}^2} = \frac{E_{no_2}^2 E_{ng}^2}{2E_{no_2}^2 - E_{no_2}^2} = E_{ng}^2 \text{ .}$$

Noise Measurement Procedure

1. Measure the total output noise.
2. Insert a calibrated noise signal to increase output noise voltage gain by +3 dB = 10 $\log_{10}$ (2/1).
3. Noise generator signal is now equal to the ENI.

II. SINE-WAVE METHOD

Figure A-1(b) shows the block diagram of the sine-wave method experiment.

Noise Measurement Procedure

1. Measure the transfer voltage gain $K_t = V_o/V_s$ (with the source impedance Z_s included), *where* V_s *is a stable sine-wave generator.*
2. Measure the total output noise.

Thus, $E_{ni} = E_{no}/K_t \approx$ ENI.

For our measurements, K_t is the total amplifier transfer voltage gain, that is, front end differential voltage gain times all the other stage voltage gains.

APPENDIX B

AMPLIFIER THEORETICAL NOISE CALCULATIONS
(From Ref. 5)

For cascaded amplifier stages (with or without feedback), the overall ENI is obtained by (refer to Fig. B-1)

$$E_{ni}^2 = E_{ns}^2 + E_{n_1}^2 + I_{n_1}^2 R_s^2 + \frac{E_{n_2}^2 + I_{n_2}^2 r_{o_1}^2}{K_{t_1}^2} + \frac{E_{n_3}^2 + I_{n_3}^2 r_{o_2}^2}{K_{t_2}^2} + \ldots ,$$

where

I_{ni} = stage i equivalent noise current, i = 1,N,
E_{ni} = stage i equivalent noise voltage, i = 1,N,
N = total number of amplifier stages,
r_{o_1} = incremental output resistance of the first stage,
K_{t_1} = transfer voltage gain of Stage 1,
r_{o_2} = incremental output resistance of Stage 2,
β_{FB} = feedback factor,
K_{t_2} = transfer voltage gain of Stage 2,
R_s = voltage source resistance, and
V_s = driving voltage source.

Because the first stage (front end preamplifier) gain of LNA 1, LNA 2, and the preamp is relatively large, the above equation predicts that their overall noise properties are influenced primarily by their first stage noise,* that is,

$$E_{ni}^2 \cong E_{ns}^2 + E_{n_1}^2 + I_{n_1}^2 R_s^2 .$$

Thus, the total ENI voltage of the LNA 1 is determined by the BB 3620 K and is a function of amplifier bandwidth and gain. Figure B-2 shows the ENI voltages for typical BB 3620 s. Therefore, LNA 1 would have a total ENI voltage of about 1 μV, rms, for a 1-kHz bandwidth with gains from 100 to 1000 V/V, and would produce an amplifier output rms noise voltage ($E_{no} = K_t E_{ni}$) of 1 V for a total LNA 1 gain of 1 000 000.0 V/V.

The total ENI for LNA 2 is (see Ref. 5, pp. 250 and 251) approximately $\sqrt{2}$ times that of a single LM381AN (Fig. B-3), where the total LM381AN ENI over a bandwidth is given by[6]

$$E_{tn} = \sqrt{(e_n^2 + E_t^2 + i_n{}^2 R_s{}^2)\,(B.W.)}$$

$$= \sqrt{[e_n^2 + (i_n R_s)^2 + 4KTR_s]\,B.W.} ,$$

*Large front end gains (for example, from photomultiplier tubes) typically are used in some systems to reduce output noise.

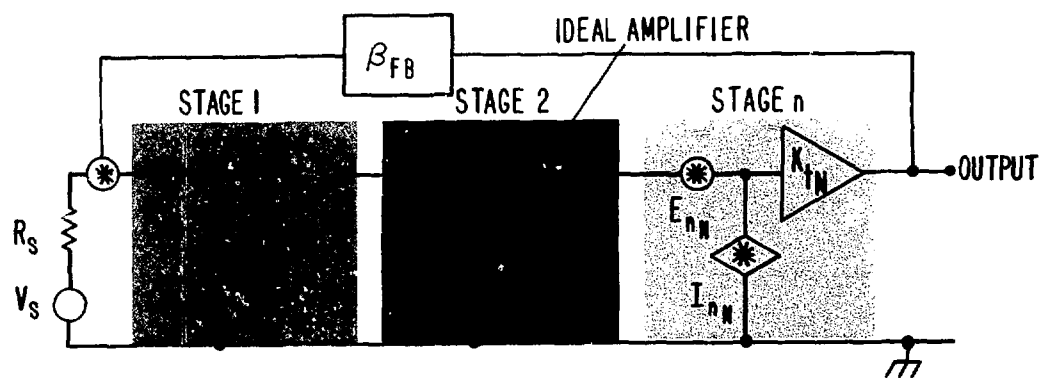

Fig. B-1.
Feedback amplifier noise model.

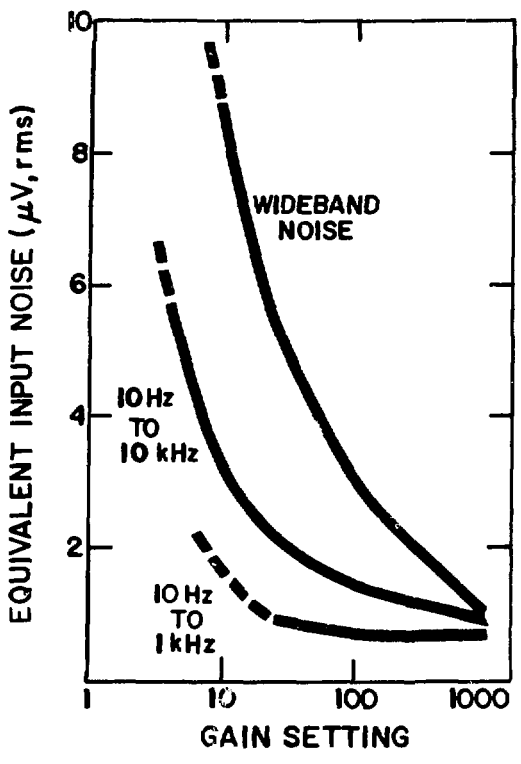

Fig. B-2.
ENI voltages for typical BB 3620 s. Note: All noise measurements were made with ***both*** *BB 3620 K inputs shorted to ground.*

where

e_n = LM381AN preamp noise voltage/$\sqrt{Hz}$ (from Ref. 6) = 3 nV/$\sqrt{Hz}$,

E_t = thermal noise produced by voltage source resistance,

i_n = LM381AN preamp noise current/$\sqrt{Hz}$ (from Ref. 6),

R_s = intrinsic thermocouple resistance = source resistance, $R_s(T) \cong$ 1-ohm average,

B.W. = amplifier bandwidth, and

T = absolute temperature (~293 K).

Therefore,

$$E_{tn} = \left\{\left[\frac{3\ nV^2}{Hz} + \left(7.2\ 10^{13}\right)^2 + 1.6566 \times 10^{20}\right] B.W.\right\}^{1/2}$$

$$E_{T_n} = 3.003\ \frac{nV\sqrt{B.W.}}{\sqrt{Hz}}\ .$$

Thus, for a noise bandwidth of 1000 Hz and a voltage gain of 10^6 V/V,

E_{T_n} = 3.003 x 31.623 = 94.9632 nV,
E_{T_n} (LNA 1) = $\sqrt{2}$ (94.9632) = 134.298 nV, and
E_{no} = 134.298 nV x 10^6 V/V = 1.343 mV rms.

If all inputs to both LM381AN channels are grounded,

$$E_{T_n} = \sqrt{(e_n^2 + 0^2 + 0^2)B.W.} = e_n\sqrt{B.W.}\ \text{and}$$

$$E_{T_n}\ (\text{LNA 1}) = \sqrt{2}e_n\sqrt{B.W.} = 134.3\ \text{nV}.$$

ACKNOWLEDGMENTS

We wish to thank the following for their contributions to this report: Richard D. Hiebert (LASL Group E-5), Ralph McFarland (LASL Group SD-5), Dennis Bohn (National Semiconductor Corporation, Santa Clara, California), and F. C. Fitchen (Dean of Engineering, University of Bridgeport, Connecticut). Our special thanks to Henry W. Johnson (LASL Group M-1) for providing the color photographs.

REFERENCES

1. C. D. Henning and R. Parker, "Transient Response of an Intrinsic Thermocouple," J. Heat Transfer **C89**, 146-154 (1967).

2. "Differential-Input Instrumentation Amplifier Model 3620," Burr-Brown Research Corporation instruction manual PDS-260c (August 1972).

3. "LF 155/LF 156/LF 157 Monolithic JFET Input Operational Amplifiers," National Semiconductor Corporation data sheets B15M95 (September 1975).

4. J. F. Pierce and J. Paulus, *Applied Electronics* (Charles E. Merrill Publishing Company, Columbus, Ohio, 1972).

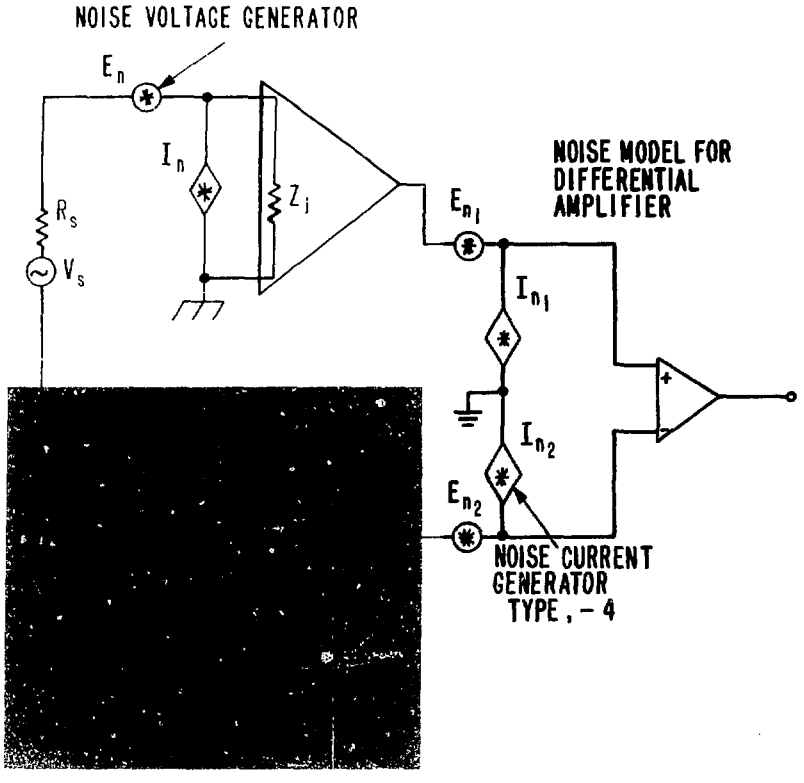

Fig. B-3.
Noise model for the instrumentation front end of the LNA 2. (Refer to front end of Fig. 5.)

5. C. D. Motchenbacher and F. C. Fitchen, *Low Noise Electronic Design* (John Wiley & Sons, Inc., New York, 1973).

6. Joe E. Byerly and Dennis Bohn, "LM381A Dual Preamplifier for Ultra Low Noise Applications," National Semiconductor Corporation application note AN-70 (April 1975).

7. F. L. Johnson, "Which—Capacitor," Marshall Industries, Capacitor Division (1955).

8. J. T. De Lorenzo, W. T. Clay, and G. C. Guerrant, "Differential Current Pulse Preamplifier for Fission Pulse Counters," IEEE Trans. Nucl. Sci. **21**, No. 1, pp. 757-762 (February 1974).

9. "2N6550 Ultra Low Noise Silicon Epitaxial Junction N-Channel Field Effect Transistor," Teledyne Crystalonics, Condensed Transistor Catalog (December 1976) p. 4.

10. "Tektronix 577-177-D1 or D2 Operators Instruction Manual," Rev. B, Tektronix, Inc., (August 1974/June 1977 reprint) p. 27.

11. Lee L. Evans, "Biasing FETs for Zero D-C Drift," Electro-Technology (August 1964).

12. Jacob Millman and Herbert Taub, *Pulse, Digital, and Switching Waveforms* (McGraw-Hill Book Co., New York, 1965).

☆ U.S. Government Printing Office: 1979 679 302